Analysis of Drone Frame

[1]Poras A. Nagmote, [2]Dr. Prashant S. Kadu, [3]Shantanu D. Munghate

[1]Student, [2]Principal, [3]Student
[1,2,3]Department of Mechanical Engineering,
[1,2,3]AGPCE, Nagpur, India.

Abstract : Frame is the structure of the drone that holds the drone together. It is essential of drone frame to be structurally strong and aerodynamically efficient. The paper investigates the arms of a multirotor drone frames as an integral and major part of drone frame for structural sustainability and aerodynamic performance. The drone arms with 5 different cross sections are analyzed viz, circular section, hollow circular section, rectangular section, triangular section, T-section and I-section. The conducted structural analysis found the hollow circular section to be optimum and conducted CFD analysis helps in concluding the fact that circular section has less aerodynamic drag and considerably less impact on lift than the rest of the sections and hence the hollow circular section is more suitable for material saving, weight reduction and has better aerodynamic performance.

Index Terms **– Drone, frame, arms, sections, hollow-circular, multirotor.**

I. INTRODUCTION:

The drone, in this case the multirotor drone is the skeleton of the multirotor assembly. The drone assembly usually consists of the motors-propeller assembly, frame, payload, electronics including flight controller, ESC's, battery and sensors. The motor-propeller assembly generates the required thrust using the power provided by the battery. This thrust in turn generates the stresses within the drone frame as it carries the entire weight of the drone. As the drone moves through the air it experiences different forces drag and lift are the predominant one. For a larger drone frame different arms cross sections are used in the arms of the drone. These sections have an aerodynamic as well as structural impact on the drone frame. The drone frame is responsible for carrying the entire weight of the drone as well as it is desired that it should contribute lesser and lesser towards the aerodynamic drag.

In this paper an attempt has been made to analyze 5 different cross sections under structural as well as aerodynamic conditions. The circular, hollow circular, rectangular, triangular, T-section and I-section being one of the most commonly found sections in drone assembly are selected as the cross sections to be analyzed. The structural analysis is done in static structural module of Ansys 19.2 while the aerodynamic analysis is done is Fluent module.

II. LITERATURE SURVEY:

Martinetti, A., Margaryan, M., & Dongen, L. van. (2018) [1] In this paper the author gives guidelines and suggestions to maintain quadcopter. On three analysis of structure and flying modes is done. First it studied about the mechanical stress on body frame using Finite Element Methods(FEM). Second analysis shows the weak points in the design to give the possible failure in mechanism of drone. Finally discussed about the performance and mechanical properties of the quadcopter.

Prajwalkumar M. Patil et al (2019) [2] The paper concentrates on modelling, analysis and fabrication of quadcopter with payload drop mechanism. The payload weight was adjusted around 5 Kg and the static, dynamic and CFD analysis were performed. The author compared three different materials which are Aluminium, carbon fibre and Balsa wood. The author advocates the use of Aluminium for his design being lightweight, cheap and strong.

Swapnil Yelmle [3] The authors focus is reducing the cost of drone frame by replacing the carbon fibre pipe frame with the aluminium frame while keeping the weight constraint. The designed frame capacity is 2.5 kg. The drone weighs about 3207 grams. The analysis in Ansys 19.2 yields 0.83 mm deformation at the motor end and 367 MPa of maximum principal stress at the centre of the frame. The obtained factor of safety is 3.

P. Jagadeeshwaran et al[4] In this paper author is numerically analysing the tilt-Hexacopter for finding out its maximum speed. The drag force and coefficient of drag is performed as an evaluation parameter. The maximum forward selected for the configuration selected by the author is 40 m/s with maximum vertical speed of 30 m/s. The variation of drag force is from 1.5 to 2 kg for 40 m/s to 45 m/s for the forward motion. While for the vertical motion is 30 m/s to 35 m/s is from 3.34069 to 4.69479 kg respectively.

Brijesh Patel et al [5] This paper deals with the static structural analysis of arms. In this analysis arm of hexacopter frame was loaded with the load at the motor end and the arm was fixed at the root. 22.94% extra volume was laid at the root in order to prevent the failure. After this change the factor of safety is found to be 2.4.

P.V.Sawalakhe, J.A. Shaaikh [6] The author concentrates on the stress concentration in the frame of UAV due to kinetic energy absorption by the UAV frame. The frame was analysed under eigen frequencies between 1.11E2 to 2.77E3 Hz and a periodic load of 3N, the arms deformation was found between 0.065 to 0.075 mm. The maximum von Mises Stress is 110MPa. The CFD analysis found the pressure to be 10E10 N/m2. Above analysis is done on the quarter frame of the UAV considering it as symmetric.

Gopichand Allaka et al [7] In this paper the multicopter is Modelled in Pro-E and analysis is done in Ansys 13.0. The structural analysis conducted with 600N load while the ultimate tensile stress obtained were 4.6E8 Pa and the maximum equivalent stress is 1.669E5 Pa for which the structure is under safety limit. The material considered for analysis is structural steel.

Muhammad A. Muflikhun et al [8] The aluminium quadcopter frame is the subject of analysis of this paper the casting type A356.0-T6.0-T6 is used to design the frame. Forces varying from 0-5 kg were used of quadcopter arms for different lengths between 34 to 234 mm were applied. The highest von mises stresses were found in the range 9.139 MPa to 74.433 MPa. While the factor of safety ranges from 16.63 to 2.04 is obtained for the length ranging from 34 to 234 mm. According to the author the aluminium frames are cheaper and are of less weight.

Kosim Abdurohman et al [9] In this paper, stress analysis of twin boom of LSU 05 UAV is done using 4 different materials viz, aluminium, e-glass fibre, carbon fibre and hybrid of aluminium and carbon fibre. The highest stress in the boom pipe and

frame near the rear end are 72.4 MPa and 118 MPa respectively and 118 MPa for skin. Stress reduction in the aluminium boom with modification is 79% and for the hybrid material is 82.9%.

Osama Jamal et al [10] In this paper, frame and propellers were considered for the structural and CFD analysis. The frame is made using 3D printing and PLA-Plus material for the dimensions bound within 24x25x10 cm volume. The inlet velocity of 130 m/s is considered for the analysis. For the following analysis max deformation, maximum elastic strain and maximum stress values for 1 N load acting on the drone are 0.00096759 mm, 0.0011151 mm/mm and 1.1498 MPa respectively. Acrylic part was used to deal with the deformation.

Seokkwan Yoon1 et al [11] The study illustrates the flow simulation for a quadrotor. The simulation results were obtained for all three motions of quadrotor. For diamond formation (X-configuration), the aerodynamic interaction between rotors while hovering a small effect on overall thrust and moments. While for pitch motion the thrust of upstream and downstream rotors was not affected much by each other the side rotors were responsible for thrust imbalance creating finite pitch and roll moments. When compared to the diamond formation, the square formation (+ configuration) shows fairly large pitching moments. The study indicates a favourable flight for the diamond formation in hover and pitch motion while the square formation remains largely influenced by aerodynamic forces.

Dhwanil Shukla et al [12] The paper focuses on nonplanar multirotor hexrotor. The paper illustrates number of different configurations for hexrotor and defines orientation and torque control. This paper theoretically derives the static mapping between demand control forces and required motor thrust. The control parameters established by the paper includes translational damping, natural frequency and angular speed damping.

III. FRAME DESIGN:

The appropriate frame structure is necessary for both the mechanical loading and reducing the aerodynamic loads. The arms cross section plays a vital role in deciding both the parameters while considering the strength and aerodynamic criteria. The most common cross sections in case of bending loads are Triangular section, I section, Rectangular section, Circular Section and T section. The literature establishes the fact that the rectangular section is the strongest section among the rest. Rather the I section will provide the required strength with material saving. While considering the aerodynamic loads the circular section can be considered as the most aerodynamically efficient. The simplified CAD model of arms of each section were created in CATIA V5 and analyzed in Ansys 19.2. The resultant of both the generated stresses and aerodynamic drag were analyzed and a section was selected for the further design.

3.1 SELECTION OF FRAME CONFIGURATION:

The Hexarotor frame configuration is selected for initial iteration. Since Hexarotor has better structural features than that of quadrotor and also the motor thrust per motor can be minimized by addition of two extra motors.

3.2 THRUST REQUIREMENT:

The Maximum payload weight to be lifted by the propulsion system is 3kg i.e. 29.43 N. The required thrust is to be divided among 6 motors. The payload weight along with the weight of assembly is to be estimated for thrust calculations. The used hexarotor weighs around 3Kg for the particular set of payload requirements and hence an overall weight of 6Kg i.e. 58.56 N is to be lifted by the propulsion system. The required thrust for maneuvering the drone is usually in the ratio 3:1. Hence, the required thrust for each motor is 3000g or 29.430 N.

3.3 SELECTION OF APPROPRIATE CROSS SECTION:

Five different cross sections were analyzed keeping the area limits same for all the cross sections and results are analyzed using Ansys Static Structural module. The boundary conditions are selected as the root of arm is selected as the fixed support and the motor base at tip is loaded with the thrust of an individual motor.

Table 3.3.1 Circular Section: Structural Analysis

Circular section	Stress MPa	Strain mm/mm	Deformation mm
Minimum	2.0734e-4	7.1495e-10	0
Maximum	10.222	5.0378e-5	0.21256
Average	1.8727	6.5008e-6	0.073274

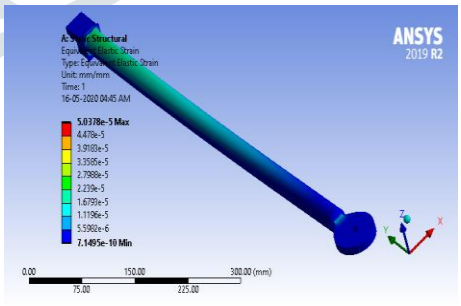

Fig 3.3.1 Circular section: Equivalent Elastic strain

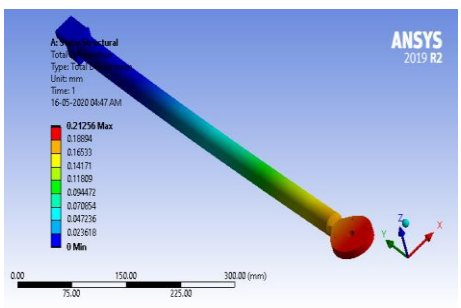

Fig 3.3.2 Circular section: Total deformation

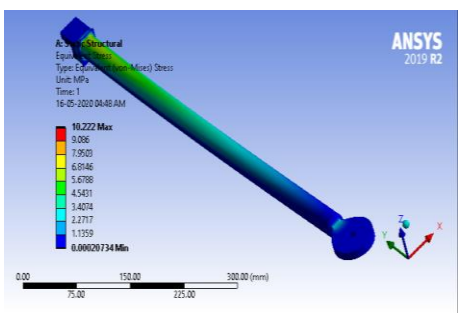

Fig 3.3.2 Circular section: Equivalent Stress

Table 3.3.2 Hollow Circular Section: Structural Analysis

Circular Hollow section	Stress MPa	Strain mm/mm	Deformation mm
Minimum	2.4359e-4	7.3933e-6	0
Maximum	10.835	6.4214e-3	0.25554
Average	2.1573	7.7327e-4	0.085564

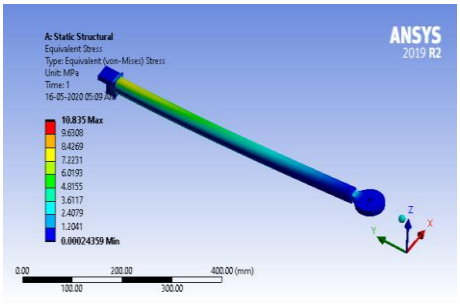

Fig 3.3.3 Circular Hollow Section: Equivalent Stress

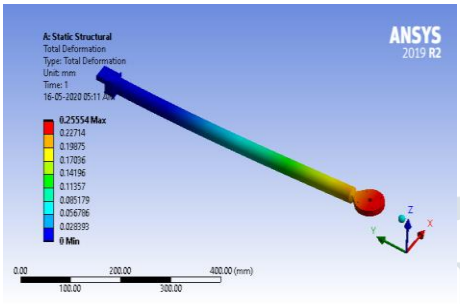

Fig 3.3.4 Circular Hollow Section: Total Deformation

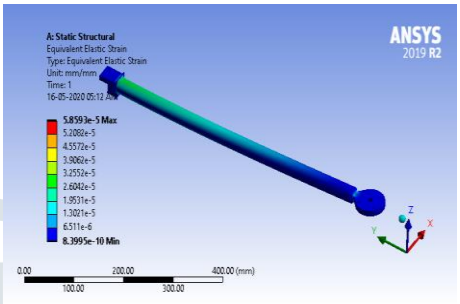

Fig 3.3.5 Circular Hollow Section: Equivalent Elastic Strain

Table 3.3.3 Rectangular Section: Structural Analysis

Rectangular section	Stress MPa	Strain mm/mm	Deformation mm
Minimum	1.7577e-4	6.0609e-10	0
Maximum	7.3375	3.4834 -5	0.12632
Average	1.1762	4.1264e -6	4.7968e-2

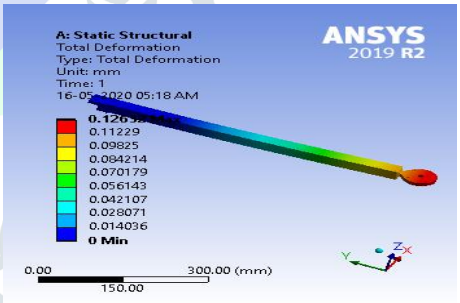

Fig 3.3.6 Rectangular Section: Total deformation

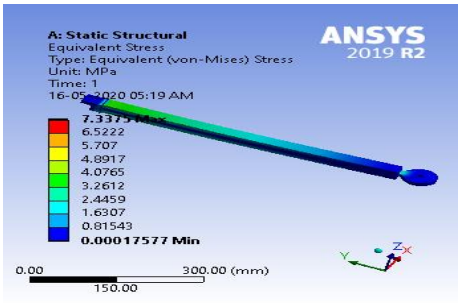

Fig 3.3. 7 Rectangular Section: Equivalent Stress

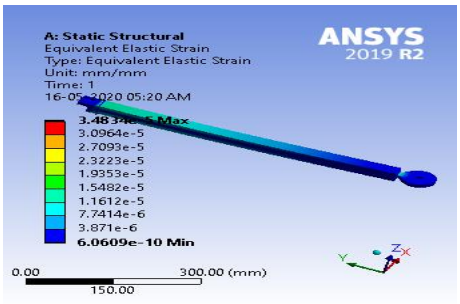

Fig 3.3.9 Rectangular Section: Equivalent Elastic Strain

Table 3.3.4 Triangular Section: Structural Analysis

Triangular-section	Stress MPa	Strain mm/mm	Deformation mm
Minimum	7.2693e-4	3.8318e-9	0
Maximum	31.05	1.0831e-4	0.37463
Average	2.3957	8.3969e-6	0.14956

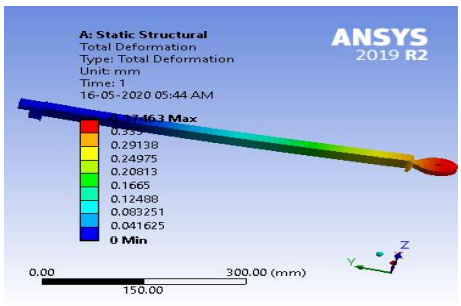

Fig 3.3.8 Triangular Section: Total Deformation

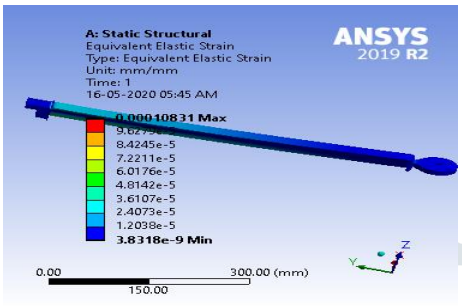

Fig 3.3.9 Triangular Section: Equivalent Stress

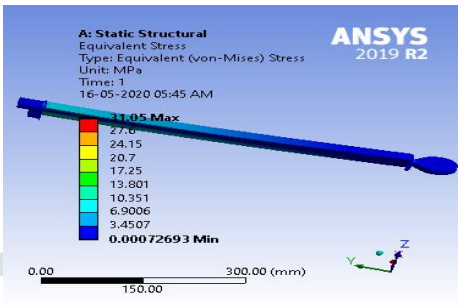

Fig 3.3.10 Triangular Section: Equivalent Elastic Strain

Table 3.3.5 T- Section: Structural Analysis

T- section	Stress MPa	Strain mm/mm	Deformation mm
Minimum	2.4421e-4	8.4209e-10	0
Maximum	20.316	7.1076e-5	0.28243
Average	1.9473	6.8055e-6	0.10776

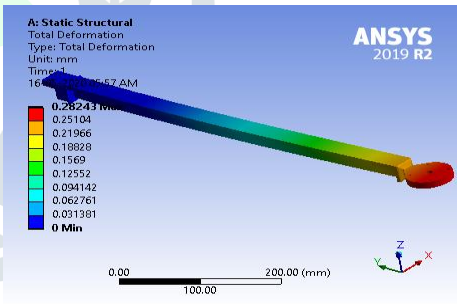

Fig 3.3.11 T-section: Total Deformation

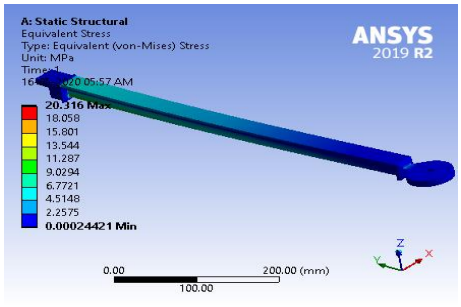

Fig 3.3.12 T-section: Equivalent Stress

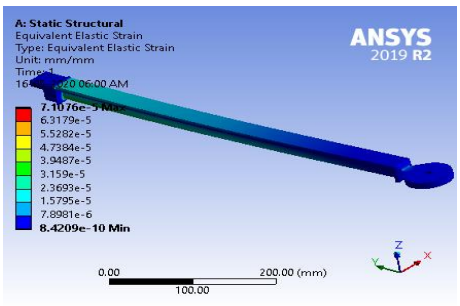

Fig 3.3.13 T-section: Equivalent Elastic Strain

Table 3.3.6 I- Section: Structural Analysis

I-section	Stress MPa	Strain mm/mm	Deformation mm
Minimum	1.0958e -4	3.7785e-10	0
Maximum	7.0713	3.7592e-5	0.1.3944
Average	1.2959	4.5243e-6	0.050431

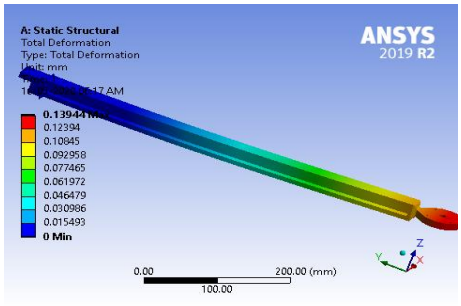

Fig 3.3.14 I-section: Total Deformation

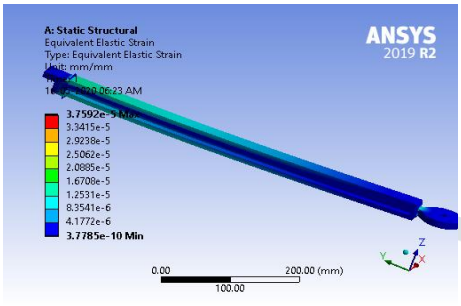

Fig 3.3.15 I-section: Equivalent Stress

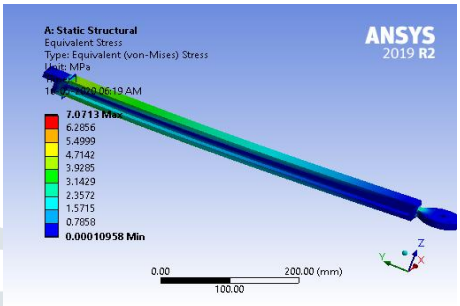

Fig 3.3.16 I-section: Equivalent Elastic Strain

3.4 Arms Aerodynamics Analysis:

To find out the appropriate cross section of the arm it is essential to find out whether the arm generates less drag under aerodynamic loads also it is crucial to find out that the arms doesn't generate a large amount of negative thrust i.e. the force opposite to the vertical force. The arms are analyzed under 45° Pitch/Roll angle which is the maximum amount of angle which can be achieved under the stable motion conditions. The relative velocity is selected based on the general air velocity (9mph=4.42m/s) and the drone operating speed restrictions (50 Kmph=14m/s). The relative velocity will be the combination of both of these velocities under 45° Pitch/Roll angle. Under Ansys Fluent, K-epsilon Realizable with Standard wall Function turbulent model was used to analyze the arms. The solutions were calculated till convergence was achieved for which the residuals were kept at 10^{-6} order.

Table 3.3.7 CFD analysis boundary Conditions

Relative velocity at flow inlet (velocity-type)	Xcomponent=0 m/s; Ycomponent=13.1254 m/s; Zcomponent=-3.1254 m/s
Outlet (pressure-type)	Gauge pressure (pressure over 101325 Pa) = 0 Pa
The Arm (wall-type)	No slip stationary wall
Flow Domain (fluid-type)	Density= 1.1845 kg/m^3 Viscosity=1.8444x10^{-5} N-s/m^2
Model	K-epsilon Realizable with Standard wall Function model, double precision and second order momentum equation.

The results were generated for all the 5 cross sections while the hollow circular cross section gave the same results as that of the solid circular cross section. The drag force contains the results of rearward drag opposite to the direction of motion created by the air while the negative thrust is the force generated opposite to the thrust force due to aerodynamic drag.

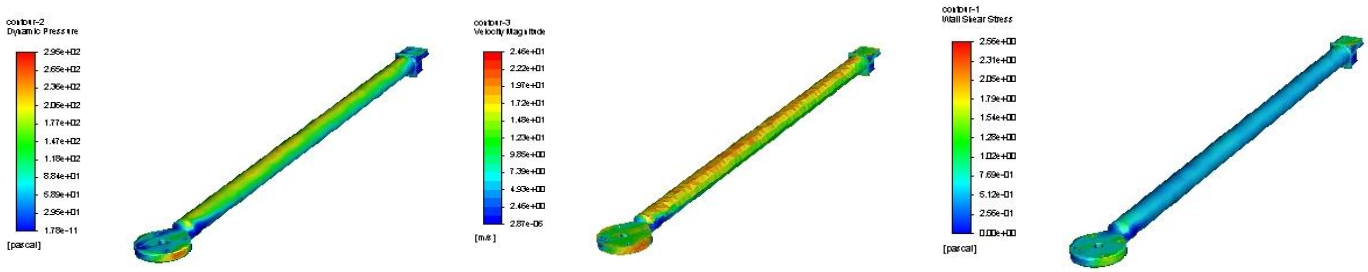

Fig 3.4.1 Circular Arm: Dynamic Pressure Fig, Circular Arm: Velocity Magnitude, Circular Arm: Wall Shear Stress

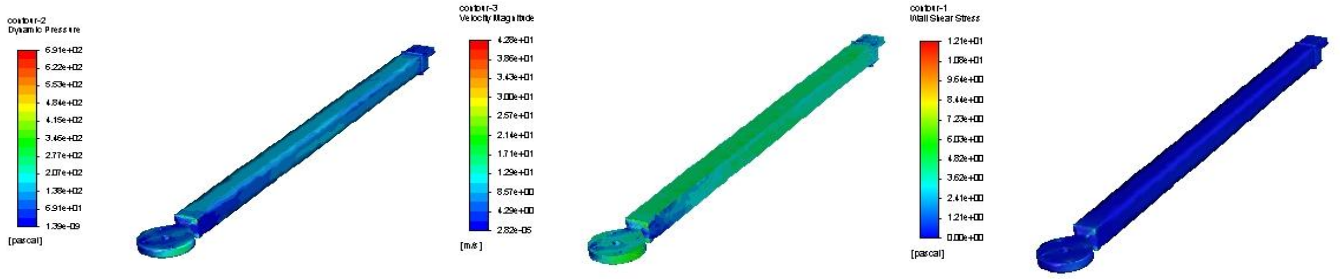

Fig 3.4.2 Rectangular Arm: Dynamic Pressure, Rectangular Arm: Velocity Magnitude, Rectangular Arm: Wall Shear Stress

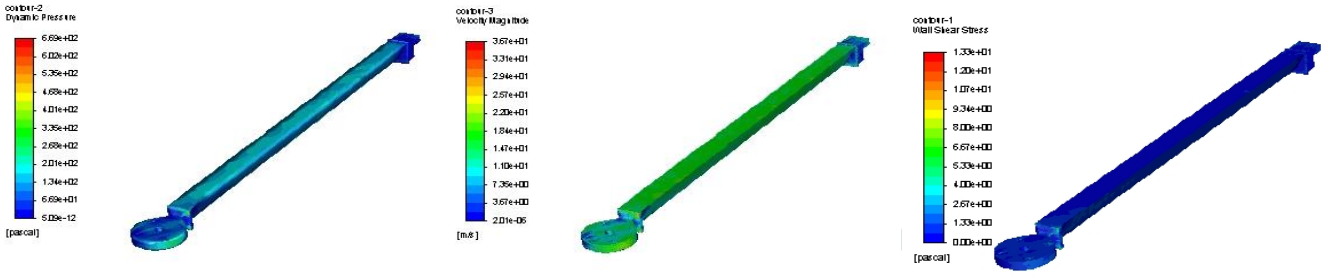

Fig 3.4.3 Triangular Arm: Dynamic Pressure, Triangular Arm: Velocity Magnitude, Triangular Arm: Wall Shear Stress

Fig 3.4.4 T-section Arm: Dynamic Pressure, T-section Arm: Velocity Magnitude, T-section Arm: Wall Shear Stress

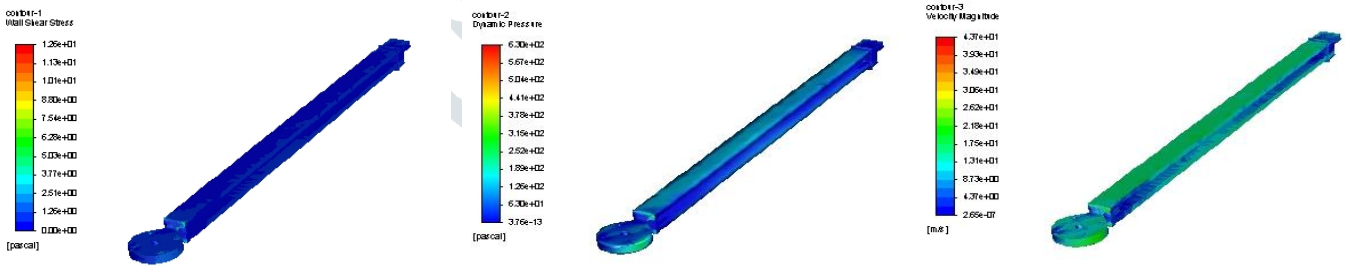

Fig 3.4.5 I-section: Dynamic Pressure, I-section: Velocity Magnitude, I-section: Wall Shear Stress

Table 3.3.8 Aerodynamic Analysis of Cross Section

Arm Section	Drag force/Area	Negative Thrust/Area
Circular/Hollow Circular Section	5.0205E-1	2.8830E-3
Rectangular Section	9.3592E-1	6.3656E-3
Triangular Section	1.0824	1.7534E-3
T-section	1.0389	2.3154E-3
I-section	9.2812E-1	6.3979E-3

CHAPTER – IV

RESULT AND DISCUSSION

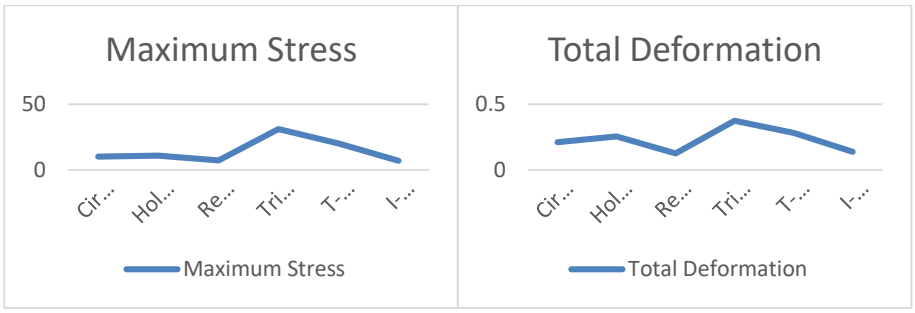

Graph 4. 1 Maximum Stress and Total Deformation vs. arm sections

The maximum stress and total deformation vs arm section graph shows that the Rectangular section is strongest followed by I section and Circular Section.

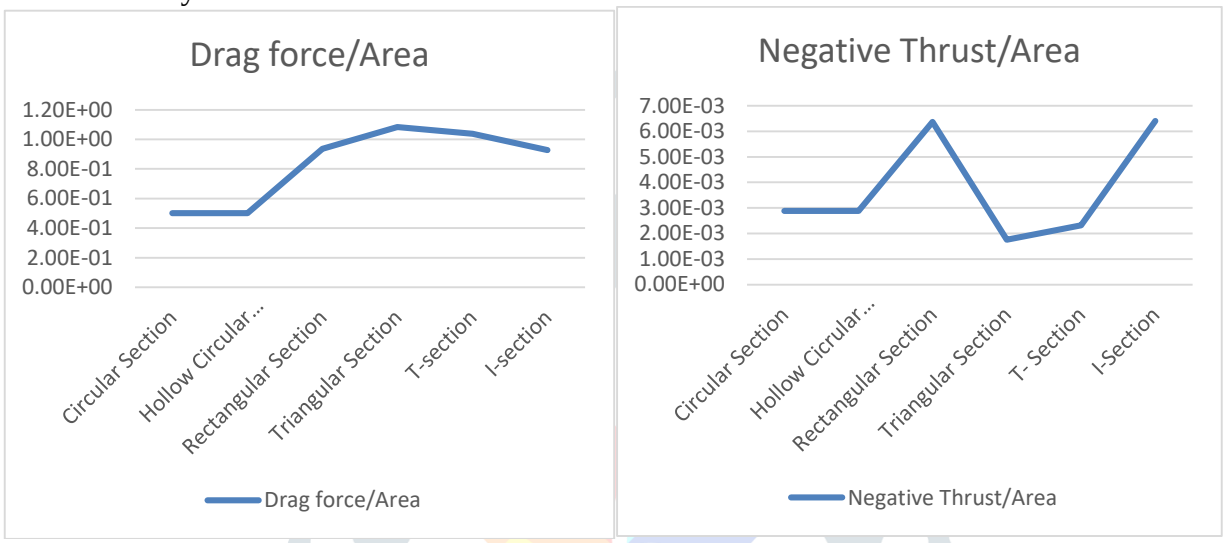

Graph 4. 2 Drag force/Area and Negative Thrust/Area vs. arm sections

While the graph of Drag force and negative thrust vs. sections shows that the circular section has the least value for both quantities. This shows that circular section can be selected. In order to reduce weight and have optimum amount of strength hollow circular section can be selected for arms.

REFERENCES

[1] Martinetti, A., Margaryan, M., & Dongen, L. van. (2018). Simulating mechanical stress on a micro Unmanned Aerial Vehicle (UAV) body frame for selecting maintenance actions. Procedia Manufacturing, 16, 61

[2] Prajwalkumar M. Patil et al, "Modeling, Analysis & Fabrication of Quadcopter (Uav) With Payload Drop Mechanism" International Journal of Research in Advent Technology, Special Issue, March 2019.

[3] Swapnil Yemle "Design & Analysis of Multi-Frame for Octo & Quad Copter Drones" International Research Journal of Engineering and Technology (IRJET) Volume: 06 Issue: 06 June 2019

[4]. P. Jagadeeshwaran et al, "Numerical Estimation of Ultimate Specification of Advanced Multi-Rotor Unmanned Aerial Vehicle" International Journal of Scientific & Technology Research Volume 9, Issue 01, January 2020

[5]. Brijesh Patel et al, "Structural Analysis of Arm of Multicopter with Various Loads", International Journal of Emerging Technology and Advanced Engineering, Volume 8, Issue 4, April 2018

[6]. P.V.Sawalakhe, J.A. Shaaikh "Simulation and Analysis of a Quadrotor UAV while Landing." International Journal of Recent Technology and Engineering (IJRTE), Volume-8 Issue-6, March 2020

[7]. Gopichand Allaka et al, "Modelling and Analysis of Multicopter Frame and Propeller" IJRET, Volume: 2 Issue: 4 APR2013.

[8]. Muhammad A. Muflikhun et al "Design of a Quadrotor UAV Aluminum Casting Frame" RCMME, HUST, Hanoi, Vietnam 2014.

[9]. Kosim Abdurohman et al "Design and Stress Analysis of LSU 05 Twin Boom Using Finite Element Method" International Seminar on Aerospace Science and Technology, At DRN Puspitek, Serpong, Tangerang, Volume: 01 November 2014

[10]. Osama Jamal et al "CFD Analysis of Quadcopter" The 4th International under-Graduate Research Conference, IUGRC 2019, July 29th -August 1st, 2019, At Cairo, Egypt.

[11] Seokkwan Yoon1 , Henry C. Lee2 , and Thomas H. Pulliam3 "Computational Analysis of Multi-Rotor Flows" 54th AIAA Aerospace Sciences Meeting USA 4-8 January 2016

[12] Dhwanil Shukla and Narayanan Komerath "Multirotor Drone Aerodynamic Interaction Investigation" MDPI journal Drones 2018, 2, 43; doi:10.3390/drones2040043